The Astrophysical Journal Letters, 765:L37 (6pp), 2013 March 10 doi:10.1088/2041-8205/765/2/L37

AN *HST*/WFC3-UVIS VIEW OF THE STARBURST IN THE COOL CORE OF THE PHOENIX CLUSTER

Michael McDonald[1,8], Bradford Benson[2], Sylvain Veilleux[3,4,5,6], Marshall W. Bautz[1], and Christian L. Reichardt[7]
[1] Kavli Institute for Astrophysics and Space Research, MIT, Cambridge, MA 02139, USA; mcdonald@space.mit.edu
[2] Kavli Institute for Cosmological Physics, University of Chicago, 5640 South Ellis Avenue, Chicago, IL 60637, USA
[3] Department of Astronomy, University of Maryland, College Park, MD 20742, USA
[4] Joint Space-Science Institute, University of Maryland, College Park, MD 20742, USA
[5] Astroparticle Physics Laboratory, NASA Goddard Space Flight Center, Greenbelt, MD 20771, USA
[6] Max-Planck-Institut für extraterrestrische Physik, Postfach 1312, D-85741 Garching, Germany
[7] Department of Physics, University of California, Berkeley, CA 94720, USA
Received 2012 November 29; accepted 2013 February 10; published 2013 February 22

ABSTRACT

We present *Hubble Space Telescope* Wide Field Camera 3 observations of the core of the Phoenix cluster (SPT-CLJ2344-4243) in five broadband filters spanning rest-frame 1000–5500 Å. These observations reveal complex, filamentary blue emission, extending for >40 kpc from the brightest cluster galaxy. We observe an underlying, diffuse population of old stars, following an $r^{1/4}$ distribution, confirming that this system is somewhat relaxed. The spectral energy distribution in the inner part of the galaxy, as well as along the extended filaments, is a smooth continuum and is consistent with that of a star-forming galaxy, suggesting that the extended, filamentary emission is not due to the central active galactic nucleus, either from a large-scale ionized outflow or scattered polarized UV emission, but rather a massive population of young stars. We estimate an extinction-corrected star formation rate of $798 \pm 42\ M_{\odot}\ \mathrm{yr}^{-1}$, consistent with our earlier work based on low spatial resolution ultraviolet, optical, and infrared imaging. The lack of tidal features and multiple bulges, combine with the need for an exceptionally massive ($>10^{11}\ M_{\odot}$) cold gas reservoir, suggest that this star formation is not the result of a merger of gas-rich galaxies. Instead, we propose that the high X-ray cooling rate of $\sim$2700 $M_{\odot}\ \mathrm{yr}^{-1}$ is the origin of the cold gas reservoir. The combination of such a high cooling rate and the relatively weak radio source in the cluster core suggests that feedback has been unable to halt cooling in this system, leading to this tremendous burst of star formation.

Key words: galaxies: active – galaxies: clusters: general – galaxies: clusters: individual (SPT-CLJ2344-4243, Phoenix) – galaxies: elliptical and lenticular, cD – galaxies: starburst

1. INTRODUCTION

In the cores of some galaxy clusters, the hot ($\gtrsim 10^7$ K) intracluster medium (ICM) can reach high enough densities that the gas should cool by a combination of thermal bremsstrahlung and line cooling in less than a Hubble time, leading to cooling flows on the order of 100–1000 $M_{\odot}\ \mathrm{yr}^{-1}$ (Fabian 1994). Much effort has been devoted to detecting these cooling flows at lower temperatures using a variety of methods. Intermediate-temperature gas has been detected in a number of clusters via spectroscopy in the X-ray (Peterson et al. 2001; Peterson & Fabian 2006), UV (e.g., O VI; Oegerle et al. 2001; Bregman et al. 2006), optical (e.g., Hα; Hu et al. 1985; Heckman et al. 1989; Crawford et al. 1999; McDonald et al. 2010), infrared (e.g., H_2; Jaffe et al. 2005; Donahue et al. 2011), and millimeter (e.g., CO; Edge 2001; Edge et al. 2002; Salomé & Combes 2003; McDonald et al. 2012b). However, even if this intermediate-temperature gas originated in the hot phase, the amount of it is orders of magnitude less than predicted by simple cooling flow models. Similarly, the star formation rate (SFR) in the brightest cluster galaxy (BCG), whether measured in the UV/optical (McNamara & O'Connell 1989; Koekemoer et al. 1999; O'Dea et al. 2004; Hicks et al. 2010; McDonald et al. 2011) or infrared (O'Dea et al. 2008; Rawle et al. 2012; Hoffer et al. 2012), only accounts for a small fraction ($\lesssim$10%) of the predicted cooling flow. While there is some evidence that this intermediate-temperature gas and low-level star formation may represent a "residual cooling flow" (e.g., Peterson & Fabian 2006; O'Dea et al. 2008; McDonald et al. 2010; Hicks et al. 2010; Tremblay et al. 2012), the fact that the majority of the X-ray-inferred cooling is unaccounted for has served as prime evidence that some form of feedback is at work in cluster cores. The exact feedback mechanism that prevents the cooling catastrophe from happening is still not fully understood. The leading hypothesis of mechanical active-galactic-nucleus-(AGN)-driven feedback is supported by the correlation between the total energy required to offset cooling and the amount of radio power required to inflate X-ray cavities (Rafferty et al. 2006; Fabian 2012; McNamara & Nulsen 2012).

Recently, McDonald et al. (2012a) reported the unique properties of a galaxy cluster at $z = 0.596$, SPT-CLJ2344-4243 (hereafter the Phoenix cluster), which was initially discovered by the South Pole Telescope using the Sunyaev–Zel'dovich effect (Williamson et al. 2011). This cluster is among the most massive ($M_{200,Y_X} \sim 2.5 \times 10^{15}\ M_{\odot}$), X-ray luminous ($L_{2-10\,\mathrm{keV}} = 8.2 \times 10^{45}$ erg s^{-1}), and strongest cooling ($\dot{M} \sim 3820\ M_{\odot}\ \mathrm{yr}^{-1}$) clusters discovered to date. The central galaxy in the Phoenix cluster appears to be experiencing a 740 $M_{\odot}\ \mathrm{yr}^{-1}$ starburst. However, it also harbors a powerful AGN which makes it difficult to separate contributions to the ultraviolet, optical, and infrared emission from star-forming regions versus the AGN in low-resolution imaging. Further, the available ground-based data optical and space-based ultraviolet (UV) and infrared (IR) data presented in McDonald et al. (2012a) were unable to distinguish between in situ star formation and the late stages of a merger.

In this Letter, we present new *Hubble Space Telescope* observations that improve significantly in depth and spatial

[8] Hubble Fellow.

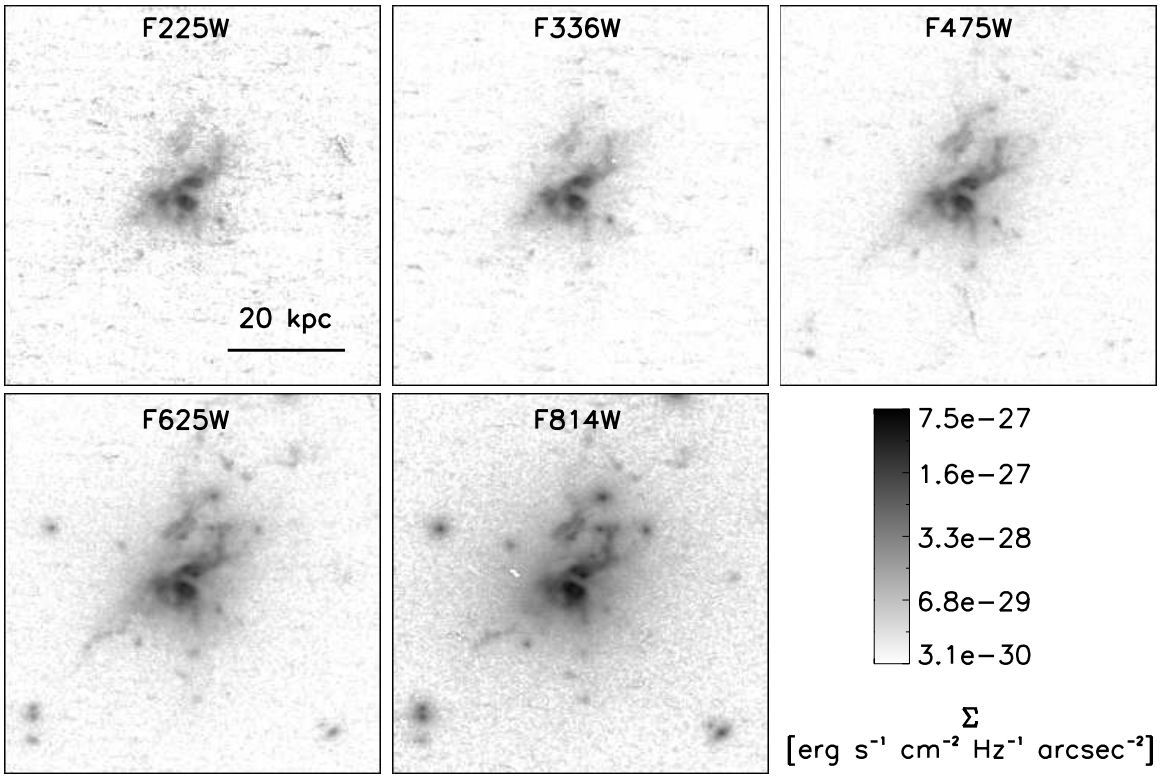

Figure 1. *HST*-WFC3 images of the core of the Phoenix cluster, in five different optical bands (rest-frame 1000–5500 Å). These images highlight the complex morphology of the BCG. The presence of extended emission in all bands argues in favor of continuum emission from young stars over line emission from ionized gas. The full extent of these filaments (∼40 kpc) is reminiscent of those observed in nearby cool core clusters such as Perseus and A1795.

resolution on the data presented in McDonald et al. (2012a). In Section 2 we describe our analysis of these data, after which we present our new, detailed view of the Phoenix cluster in Section 3. In Section 4 we discuss the possible interpretations of these data, including whether or not we can separate the cooling flow scenario from a pure AGN or merger scenario. We conclude with a summary of these results in Section 5. Throughout this Letter we assume $H_0 = 70$ km s^{-1} Mpc^{-1}, $\Omega_M = 0.27$, and $\Omega_\Lambda = 0.73$.

2. *HST* DATA

To study in detail the purported starburst in the core of the Phoenix cluster, we obtained broadband imaging with the *Hubble Space Telescope* Wide Field Camera 3 (*HST* WFC3) in five optical filters—F225W, F336W, F475W, F625W, F814W—which span rest-frame wavelengths from ∼1000 Å to ∼5500 Å. These observations were carried out over two orbits of Director's Discretionary Time, with an average exposure time of ∼1800 s per filter (PID 13102, PI: McDonald).

In each filter, a series of two dithered exposures were obtained. The LA Cosmic[9] (van Dokkum 2001) software was run on individual exposures, generating accurate cosmic ray and bad pixel masks for each image. Pairs of exposures were then combined using the PyRAF astrodrizzle routine,[10] with the aforementioned masks preceding the standard cosmic ray detection in the multidrizzle task. The final cleaned images are presented in Figure 1.

All optical and UV fluxes were corrected for Galactic extinction following Cardelli et al. (1989) using a Galactic reddening estimate of $E(B-V) = 0.017$ toward the cluster center, from Schlegel et al. (1998).

3. RESULTS

In Figure 1 we show the newly acquired far-UV through optical *HST* images of the core of the Phoenix cluster, which provide a detailed picture of this system. These images show significant, extended filamentary emission at all wavelengths from ∼1000–5500 Å, overlaid on a relatively smooth population of older red stars. The most extended pair of filaments to the north of the BCG are ∼6″ (40 kpc) in length, similar to the most extended filaments seen in A1795 (McDonald & Veilleux 2009), and the Perseus cluster (Conselice et al. 2001; Fabian et al. 2008). We measure a total rest-frame far-UV flux density of $f_{\rm F225W} = 1.26 \times 10^{-27}$ erg s^{-1} cm^{-2} Hz^{-1}, consistent with the *GALEX*-derived flux presented in McDonald et al. (2012a).

The fact that such complex, filamentary morphology is present in all five filters suggests that the BCG is forming stars at a prodigious rate. In the wavelength range covered, there may be contributing emission from the C IV λ1549 (F225W), [O II] (F625W), and [O III] and Hβ (F814W) lines. However, the F336W and F475W bands, which have similar surface brightnesses to the other three bands, should be relatively free from emission lines, suggesting that young stars, not ionized gas, are the dominant source of the observed flux in Figure 1.

In Figure 2 we show a three-color (F475W, F625W, F814W) image of the cluster core. This figure shows a clear difference in the stellar populations between the young (blue) filaments and the underlying, smoothly distributed, old (red) stars. The peak of the emission in all bands is coincident (within the positional uncertainties) with the X-ray point source. To the northwest and southeast of the emission peak are dark lanes, most

[9] http://www.astro.yale.edu/dokkum/lacosmic/
[10] http://www.stsci.edu/hst/HST_overview/drizzlepac

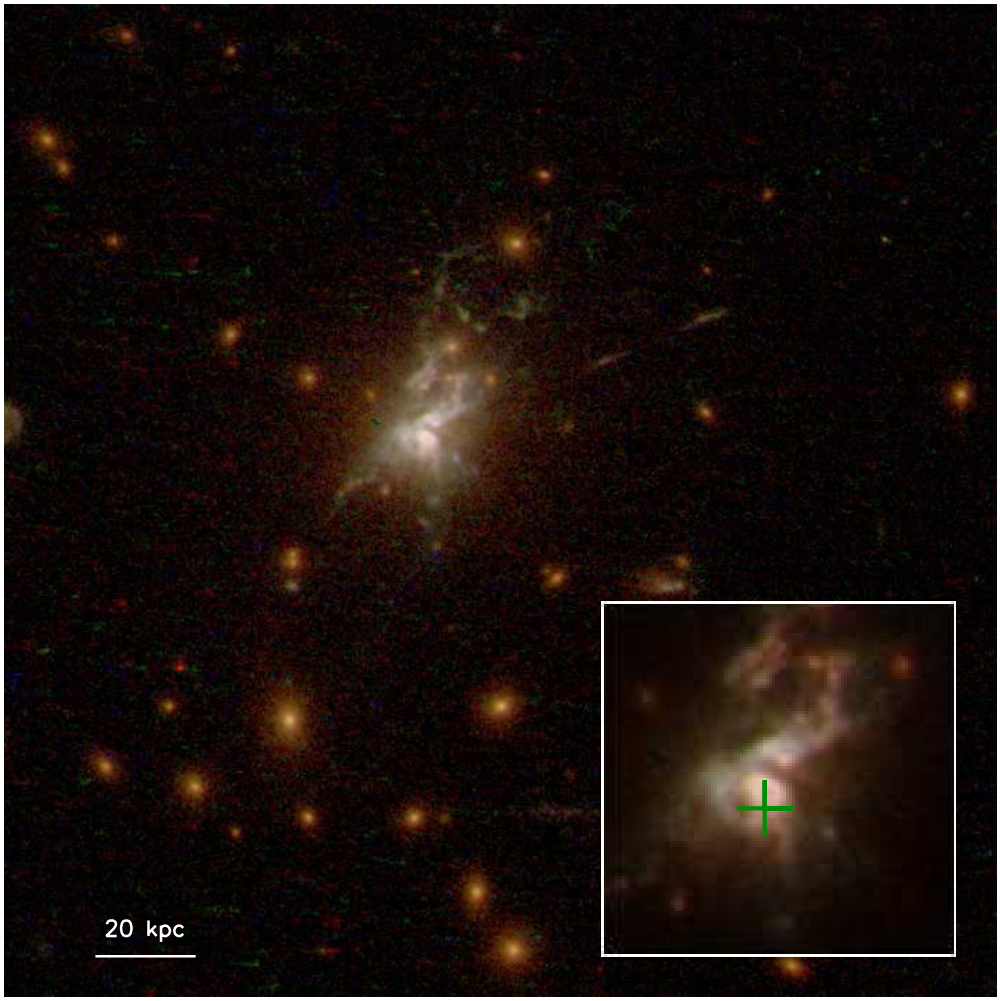

Figure 2. Color image, combining the F475W, F625, and F814W bands, showing the young, filamentary, star-forming regions overlaid on the diffuse, old stellar component of the BCG. The most extended filaments in this complex system extend for ∼40 kpc to the north and northwest of the cluster center. The linear, radial feature to the northwest has colors consistent with the rest of the filaments, suggesting that it is neither a jet nor a background lensed galaxy. In the inset we show the central ∼20 kpc, with the position (and uncertainty) of the X-ray point source in green. There appear to be gaps in the emission to the northwest and southeast of the peak, possibly due to strong dust lanes.

likely due to obscuration by dust. Overall, the color of the filamentary emission appears roughly constant with radius, and is reminiscent of a young, star-forming galaxy. We see no evidence for multiple bulges or tidal features, both of which would indicate that this system is the result of a recent merger of gas-rich galaxies.

Figure 3 shows the multi-band surface brightness profiles of the BCG (left panel), which have been computed along radial cuts at four different angles (90°, 120°, 180°, 210°), chosen to avoid the blue filamentary emission. The radial surface brightness profile follows an $r^{1/4}$ profile, which is typical of relaxed, early-type galaxies (de Vaucouleurs 1948). Such $r^{1/4}$ surface brightness distributions are also common in the final stages (single-nucleus) of low-redshift ($z < 0.3$) gas-rich mergers ultraluminous infrared galaxies (ULIRGs; e.g., Veilleux et al. 2002, 2006). However, with a half-light radius of ∼17 kpc and a stellar mass of $\sim 3 \times 10^{12}\ M_{\odot}$ (McDonald et al. 2012a), this BCG is a factor of ∼4 larger in size (Veilleux et al. 2002), a factor of ∼60 higher in stellar mass (Veilleux et al. 2006), and resides in an environment ∼50–100 times richer (Zauderer et al. 2007) than normal for $z < 0.3$ ULIRGs. Projecting these one-dimensional profiles back onto the sky, we can separate diffuse, giant elliptical emission (middle panel) from clumpy, star-forming emission (right panel). The lack of smooth, arcing tidal features and multiple bulges in the residual image (right panel) suggests that this complex, extended emission did not originate from a recent merger with one or more gas-rich disk galaxies. All of these factors argue that the Phoenix BCG is unlike a traditional ULIRG by any definition other than the high total infrared luminosity.

In Figure 4 we provide the spectral energy distribution (SED) in several representative regions around the BCG. The diffuse emission at large and small radii indicate a significant positive age gradient in the diffuse population. At large ($r \sim 40$ kpc) radii, the diffuse emission is qualitatively consistent with a 2–5 Gyr old elliptical galaxy, while at smaller radii (∼20 kpc) the diffuse stellar populations appear to be much younger (bluer), similar in color to a star-forming spiral galaxy. The extended, morphologically complex filaments, after subtraction of the diffuse stellar component, show an excess of UV emission at all radii. The SED of the brightest filaments appear remarkably similar to the diffuse component in the central region, suggesting that these stars are being mixed on short timescales. In the faintest, most extended filaments, there is a substantial excess of emission in the F225W and F625W filters, at the location of the redshifted C IV λ1549 and [O II] lines, respectively, suggesting

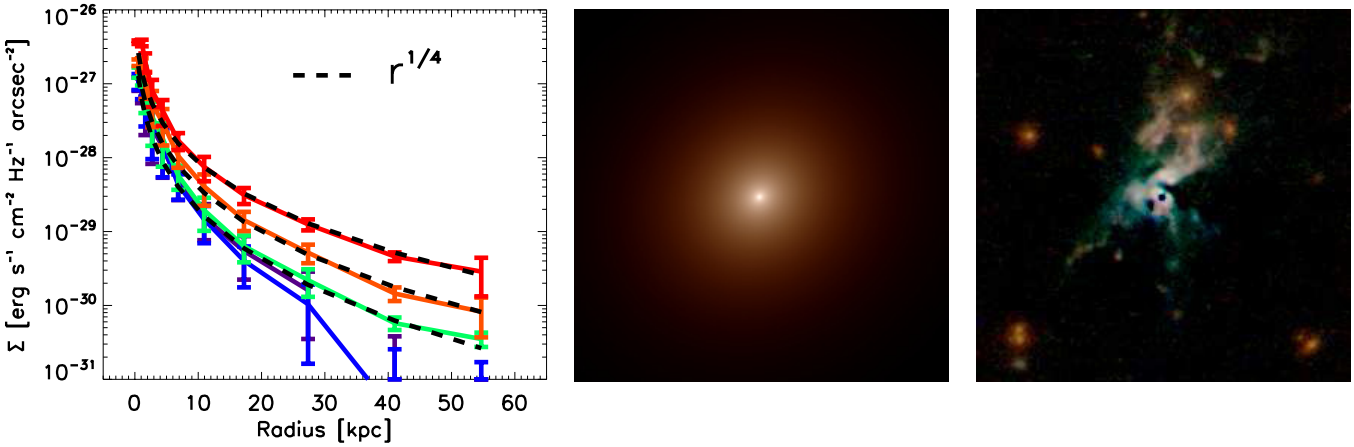

Figure 3. Left: surface brightness profiles of the BCG in all five bands (purple: F225W, blue: F336W, green: F475W, orange: F625W, red: F814W). Each profile represents the average along four radial cuts with orientations chosen to avoid most of the extended filamentary emission. The diffuse, red component of the BCG has a surface brightness distribution typical of an elliptical galaxy, well modeled by a $r^{1/4}$ falloff in surface brightness (dashed line; de Vaucouleurs 1948). Middle: two-dimensional surface brightness model from GALFIT (Peng et al. 2010), with ellipticity and PA of 0.88 and −52°, respectively. Right: residual image generated by subtracting the $r^{1/4}$ model from each of the three reddest bands. Both color images use the same color scaling as Figure 2. This figure highlights the complex morphology of the star-forming filaments superimposed on the smooth, old stellar population in the BCG.

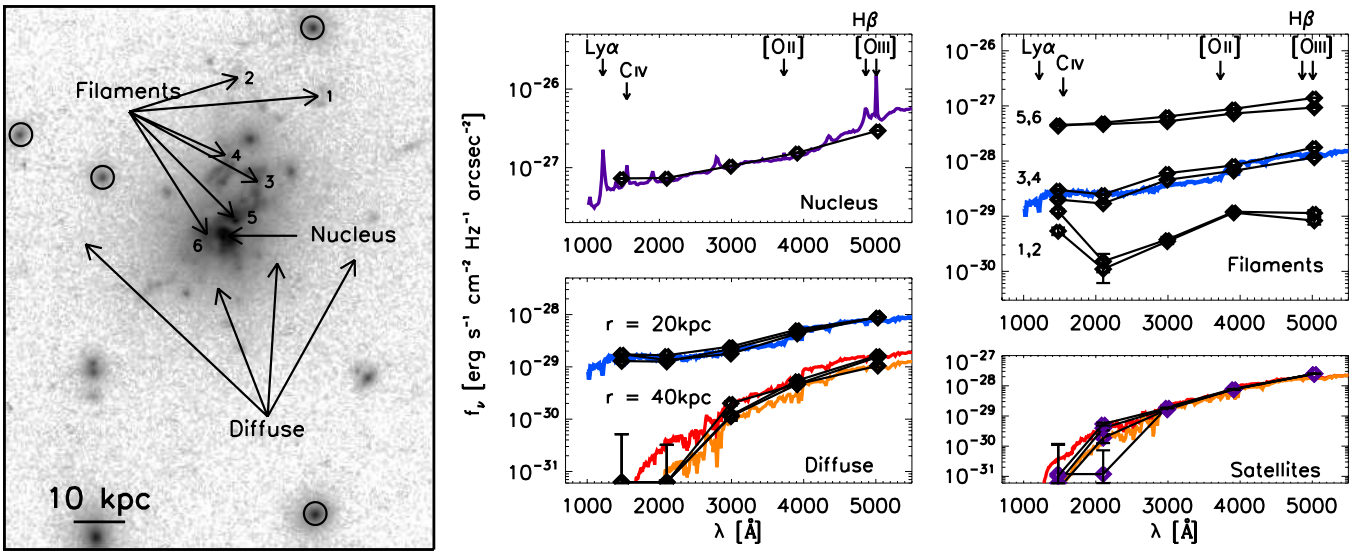

Figure 4. Left: F814W image of the Phoenix BCG, with positions of nucleus, filaments, and diffuse emission indicated. Right: SEDs for the regions indicated on the left. For comparison, we show the SEDs for four early-type satellite galaxies (marked by circles in the left panel) which have been normalized to a single value of $f_{5000\,\text{Å}}$. Orange and red spectra correspond to passive stellar populations of ages 2 and 5 Gyr, respectively, while blue and purple spectra correspond to a typical late-type spiral galaxy (Sdm) and dusty type-2 QSO, respectively (Polletta et al. 2007). All model spectra are normalized by eye and are meant to demonstrate the qualitative agreement in spectral shape. The faintest (labels 1,2) filaments show evidence for nebular emission, with peaks in the F225W and F625W bands, consistent with C IV and [O II] emission. This figure suggests that, at large radii the diffuse stellar populations are typical for an early-type galaxy, while at small radii both the diffuse and filamentary emission result from significantly younger stellar populations.

that these filaments may also contain warm ($>10^4$ K), ionized gas—a scenario supported by the extended emission lines reported in McDonald et al. (2012a). The overall flatness of the SED in the UV-bright regions is exactly what one would expect for a mix of young stars and warm, ionized gas, given the width of the broadband filters. At the peak of the optical emission, coincident with the X-ray source, the SED is qualitatively well matched by a dusty type-2 QSO (Polletta et al. 2007), which is consistent with our X-ray observations of a highly reddened hard X-ray point source.

The combination of Figures 1–4 paint a picture of an old, giant elliptical galaxy that is experiencing a resurgence of star formation. Below we re-evaluate the SFR in this system and describe various scenarios to explain this star-forming activity, building on the discussion of McDonald et al. (2012a).

4. DISCUSSION

The deep, high spatial resolution *HST* UV and optical imaging presented in Section 3 have revealed an exceptionally complex system. Below we utilize this improved spatial resolution to estimate a new, UV-derived SFR for the BCG in the Phoenix cluster, followed by a discussion of three possible origins for the extended, filamentary UV emission.

4.1. A Revised Estimate of the SFR

The SFR reported in McDonald et al. (2012a), while utilizing an array of multi-wavelength data, necessarily required multiple assumptions to remove AGN contamination. With the addition of high-resolution *HST* UV imaging, we avoid such

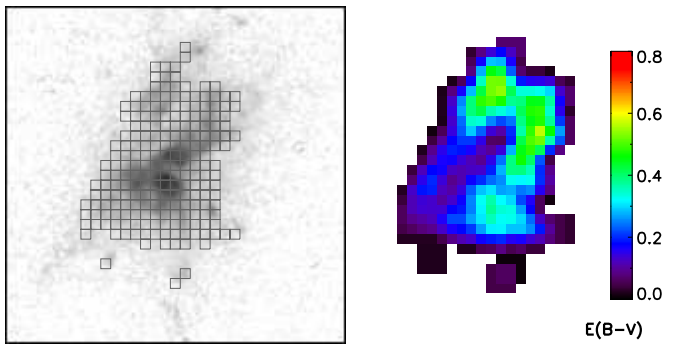

Figure 5. Left: image in the F475W band, with $0\farcs2 \times 0\farcs2$ bins overlaid in regions with $>5\sigma$ detections in both the F336W and F475W bands. Right: smoothed reddening map, derived assuming a flat UV SED in the absence of reddening (Kennicutt 1998). This map allows us to perform *local* reddening corrections on the UV images, yielding a more tightly constrained estimate of the extinction-corrected UV luminosity.

assumptions, leaving only the (typical) assumptions of dust extinctions and star formation laws.

To estimate the reddening, we assume that the reddening-free SED is flat at 1500–3000 Å (Kennicutt 1998). Since the F225W filter may be contaminated by C IV emission, we use the mean $f_{\rm F336W}/f_{\rm F475W}$ (rest frame f_{210}/f_{298}) flux ratio to derive a reddening correction, assuming $f_{\rm F336W}/f_{\rm F475W} = 1$ for $E(B-V) = 0$. In Figure 5 we show the spatial distribution of the reddening, $E(B-V)$, over regions with significant signal-to-noise (S/N > 5) UV flux. We note that the mean reddening in this map agrees well with the reddening presented in McDonald et al. (2012a) from Balmer line ratios ($E(B-V) = 0.34$). Using the *local* reddening correction and uncertainty we can accurately correct the UV luminosity, resulting in a more confident estimate of $L_{2000} = 5.7 \pm 0.3 \times 10^{30}$ erg s^{-1} Hz^{-1} and a UV-derived SFR of $798 \pm 42\ M_\odot$ yr^{-1} (Kennicutt 1998). Given the near-IR-estimated stellar mass of $M_* \sim 3 \times 10^{12}\ M_\odot$ (McDonald et al. 2012a), this high SFR implies that in 100 Myr the central galaxy in the Phoenix cluster will form 2%–3% of its stellar mass.

We note that this estimate is consistent with the AGN-subtracted SFR quoted in McDonald et al. (2012a) of $739 \pm 160\ M_\odot$ yr^{-1} and with the empirical, extinction-implicit, method of Rosa-González et al. (2002), which yields $\mathrm{SFR_{UV}} = 1040^{+1290}_{-580}\ M_\odot$ yr^{-1}.

4.2. Possible Sources of Extended UV Emission

4.2.1. AGN-driven Outflow and Scattered Light

Inspired by the high far-infrared luminosity, coupled with the hard X-ray and radio source, a viable explanation for this system is a dusty AGN driving a large-scale outflow. While there is undoubtedly a powerful AGN in the core of the Phoenix cluster, the new *HST* data suggest that the substantial UV luminosity cannot be fully attributed to a point-like AGN. Only a small fraction (<10%) of the total UV luminosity originates from a central point source, with the majority originating from extended, filamentary regions. Furthermore, the high relative fluxes in the F336W and F475W bands, which should be free from line emission, suggest that the majority of the UV/optical flux in these complex filaments is continuum emission. We also find a general lack of UV/blue emission along the minor axis of the central galaxy, contrary to what is typically observed in wide-angle AGN-driven outflows (Veilleux et al. 2005). Thus, we argue that the filamentary UV emission does not result from an outflow.

In IRAS 09104+4109 (e.g., O'Sullivan et al. 2012), along with other powerful radio galaxies, much of the extended UV continuum is due to scattered, polarized light from a heavily obscured QSO. However, the UV continuum in IRAS 09104+4109 is ∼20 times fainter than that presented here for the Phoenix cluster (Hines et al. 1999). Considering the fact that IRAS 09104+4109 is already an extreme system, it seems unlikely that this additional factor of 20 can be accounted for with the same model.

4.2.2. Gas-rich Merger(s)

The majority of known ULIRGs appear to be late-stage mergers of gas-rich galaxies (∼95%; Veilleux et al. 2002), which begs the question: Is the extreme star formation in the core of the Phoenix cluster fueled by a gas-rich merger? Assuming a relation between molecular gas depletion time and specific SFR (Saintonge et al. 2011), we estimate an H_2 depletion time of $2\text{–}12 \times 10^8$ yr, which is consistent with those measured in two nearby cooling flows: A1068 (4×10^8 yr; Edge 2001) and A1835 (5×10^8 yr; Edge 2001). Assuming a one-to-one correspondence between the total mass of stars formed and the mass of the cold gas reservoir, this timescale implies a molecular gas mass of $1.5\text{–}9.5 \times 10^{11}\ M_\odot$, consistent with more recent work by Combes et al. (2012), yielding $1.0\text{–}5.0 \times 10^{11}\ M_\odot$. This cold gas mass is significantly higher than that measured for gas-rich galaxies in the Virgo Cluster (e.g., Corbelli et al. 2012). Further, the process of increasing the cold gas content by compressing atomic gas during a merger would be highly inefficient in the core of the Phoenix cluster due to ram pressure stripping of the H I disk during the initial galaxy infall—a process observed in the Virgo Cluster, which has an ICM density ∼10 times lower than Phoenix.

4.2.3. Cooling of the Intracluster Medium

Our preferred explanation in McDonald et al. (2012a) was that the star formation in the cluster core is fueled by gas cooling out of the ICM. This remains the most plausible avenue for such a large amount of cold gas to reach the core of the cluster, and is supported by the exceptionally bright X-ray cool core and relatively weak radio source. Such an imbalance between cooling and feedback could lead to rapid cooling of the ICM, fueling bursts of star formation.

Following White et al. (1997), we estimate from the X-ray data the mass deposition rate of the cooling flow, combining the X-ray cooling luminosity with the gravitational potential of the cluster in order to correct for gravitational work done as the gas falls toward the cluster center. We obtain an ICM cooling rate of $\dot{M} = 2700 \pm 700\ M_\odot$ yr^{-1} which is enough to fuel a $798\ M_\odot$ yr^{-1} starburst, assuming the feedback mechanism that prevents star formation in nearby clusters is operating less efficiently in Phoenix. In the future, high-resolution X-ray spectroscopy of the cool core (e.g., Peterson & Fabian 2006) will provide firm estimates of the ICM cooling rate down to low temperatures, revealing whether or not this scenario is a plausible fuel source for this massive starburst.

5. SUMMARY AND CONCLUSIONS

We report new *HST* observations of the Phoenix cluster (SPT-CLJ2344-4243) with WFC3-UVIS in five filters covering rest-frame wavelengths 1000–5500 Å. The high spatial resolution of *HST* is able to separate bright UV emission from the

AGN and the surrounding diffuse extended emission, definitively confirming the presence of a starburst in the BCG. The morphology of this central galaxy is complex, with narrow filaments extending for >40 kpc, reminiscent of the nearby Perseus and A1795 clusters. We argue that the majority of the observed UV emission is due to young stars, on the basis of the complex morphology and flat SED over the wavelength range 1000–5500 Å. We confirm the high SFR presented in McDonald et al. (2012a), measuring an extinction-corrected, AGN-removed UV-derived SFR of $798 \pm 42\,M_{\odot}$ yr^{-1}. We find that merger-driven scenarios would require an unreasonably large number of gas-rich galaxies to supply the cold gas reservoir required to fuel the starburst, and conclude that the starburst is likely fueled by a massive cooling flow.

We thank the *HST* Director for graciously providing the data for this program. M.M. acknowledges support provided by NASA through a Hubble Fellowship grant from STScI. S.V. acknowledges support from a Senior NPP Award held at NASA-GSFC and from the Humboldt Foundation to fund a long-term visit at MPE in 2012. B.A.B. is supported by the National Science Foundation through grant ANT-0638937, with partial support provided by NSF grant PHY-1125897, the Kavli Foundation, and Chandra Award Number 13800883 issued by the CXC.

REFERENCES

Bregman, J. N., Fabian, A. C., Miller, E. D., & Irwin, J. A. 2006, ApJ, 642, 746
Cardelli, J. A., Clayton, G. C., & Mathis, J. S. 1989, ApJ, 345, 245
Combes, F., Garcia-Burillo, S., Braine, J., et al. 2012, arXiv:1209.5523
Conselice, C. J., Gallagher, J. S., III, & Wyse, R. F. G. 2001, AJ, 122, 2281
Corbelli, E., Bianchi, S., Cortese, L., et al. 2012, A&A, 542, A32
Crawford, C. S., Allen, S. W., Ebeling, H., Edge, A. C., & Fabian, A. C. 1999, MNRAS, 306, 857
de Vaucouleurs, G. 1948, AnAp, 11, 247
Donahue, M., de Messières, G. E., O'Connell, R. W., et al. 2011, ApJ, 732, 40
Edge, A. C. 2001, MNRAS, 328, 762
Edge, A. C., Wilman, R. J., Johnstone, R. M., et al. 2002, MNRAS, 337, 49
Fabian, A. C. 1994, ARA&A, 32, 277
Fabian, A. C. 2012, ARA&A, 50, 455
Fabian, A. C., Johnstone, R. M., Sanders, J. S., et al. 2008, Natur, 454, 968
Heckman, T. M., Baum, S. A., van Breugel, W. J. M., & McCarthy, P. 1989, ApJ, 338, 48
Hicks, A. K., Mushotzky, R., & Donahue, M. 2010, ApJ, 719, 1844
Hines, D. C., Schmidt, G. D., Wills, B. J., Smith, P. S., & Sowinski, L. G. 1999, ApJ, 512, 145
Hoffer, A. S., Donahue, M., Hicks, A., & Barthelemy, R. S. 2012, ApJS, 199, 23
Hu, E. M., Cowie, L. L., & Wang, Z. 1985, ApJS, 59, 447
Jaffe, W., Bremer, M. N., & Baker, K. 2005, MNRAS, 360, 748
Kennicutt, R. C., Jr. 1998, ARA&A, 36, 189
Koekemoer, A. M., O'Dea, C. P., Sarazin, C. L., et al. 1999, ApJ, 525, 621
McDonald, M., Bayliss, M., Benson, B. A., et al. 2012a, Natur, 488, 349
McDonald, M., & Veilleux, S. 2009, ApJL, 703, L172
McDonald, M., Veilleux, S., Rupke, D. S. N., & Mushotzky, R. 2010, ApJ, 721, 1262
McDonald, M., Veilleux, S., Rupke, D. S. N., Mushotzky, R., & Reynolds, C. 2011, ApJ, 734, 95
McDonald, M., Wei, L. H., & Veilleux, S. 2012b, ApJL, 755, L24
McNamara, B. R., & Nulsen, P. E. J. 2012, NJPh, 14, 055023
McNamara, B. R., & O'Connell, R. W. 1989, AJ, 98, 2018
O'Dea, C. P., Baum, S. A., Mack, J., Koekemoer, A. M., & Laor, A. 2004, ApJ, 612, 131
O'Dea, C. P., Baum, S. A., Privon, G., et al. 2008, ApJ, 681, 1035
Oegerle, W. R., Cowie, L., Davidsen, A., et al. 2001, ApJ, 560, 187
O'Sullivan, E., Giacintucci, S., Babul, A., et al. 2012, MNRAS, 424, 2971
Peng, C. Y., Ho, L. C., Impey, C. D., & Rix, H.-W. 2010, AJ, 139, 2097
Peterson, J. R., & Fabian, A. C. 2006, PhR, 427, 1
Peterson, J. R., Paerels, F. B. S., Kaastra, J. S., et al. 2001, A&A, 365, L104
Polletta, M., Tajer, M., Maraschi, L., et al. 2007, ApJ, 663, 81
Rafferty, D. A., McNamara, B. R., Nulsen, P. E. J., & Wise, M. W. 2006, ApJ, 652, 216
Rawle, T. D., Edge, A. C., Egami, E., et al. 2012, ApJ, 747, 29
Rosa-González, D., Terlevich, E., & Terlevich, R. 2002, MNRAS, 332, 283
Saintonge, A., Kauffmann, G., Wang, J., et al. 2011, MNRAS, 415, 61
Salomé, P., & Combes, F. 2003, A&A, 412, 657
Schlegel, D. J., Finkbeiner, D. P., & Davis, M. 1998, ApJ, 500, 525
Tremblay, G. R., O'Dea, C. P., Baum, S. A., et al. 2012, MNRAS, 424, 1042
van Dokkum, P. G. 2001, PASP, 113, 1420
Veilleux, S., Cecil, G., & Bland-Hawthorn, J. 2005, ARA&A, 43, 769
Veilleux, S., Kim, D.-C., Peng, C. Y., et al. 2006, ApJ, 643, 707
Veilleux, S., Kim, D.-C., & Sanders, D. B. 2002, ApJS, 143, 315
White, D. A., Jones, C., & Forman, W. 1997, MNRAS, 292, 419
Williamson, R., Benson, B. A., High, F. W., et al. 2011, ApJ, 738, 139
Zauderer, B. A., Veilleux, S., & Yee, H. K. C. 2007, ApJ, 659, 1096